Revue Roumaine de Chimie, **2009**, *54*(9), 773–778

FABRICATION AND CHARACTERISTICS OF VARIABLE CRYSTALLINE TiO_2 FOR PHOTOCATALYTIC ACTIVITIES

Jae Young BAE,[a]* Tae Kwan YUN,[a] Sung Soo HAN,[b] Byung Gil MIN,[c] Imre BAKO[d] and Soong-Hyuck SUH[a]

[a] Department of Chemistry and Chemical Engineering, Keimyung University, Daegu 704-701, Korea
[b] School of Textiles, Yeungnam University, Gyeongsan 712-749, Korea
[c] Department of Nano-Bio Textile Engineering, Kumoh National Institute of Technology, Gumi 730-701, Korea
[d] Department of Theoretical Chemistry, Chemical Research Center, Hungarian Academy of Sciences, Budapest H-1025, Hungary

Received September 25, 2008

Nanocrystalline TiO_2 powders with the different anatase/rutile ratios and the high surface area have been prepared using $TiCl_4$ by the precipitation method. The samples were characterized by X-ray diffraction, N_2-sorption, and UV-VIS diffuse reflectance spectra techniques. The contents of anatase and rutile phases in TiO_2 powders have been successfully controlled by simply changing the proportion of SO_4^{2-} and Cl^- ions in the aqueous solution. The photodegradation of congo red in water has been investigated over the wide range of TiO_2 for different anatase/rutile ratios in visible region. The catalysts containing 19.7% rutile showed the highest photocatalytic activity in our study.

INTRODUCTION

Since the discovery of photoelectrochemical splitting of water on TiO_2 electrodes,[1] titania has attracted extensive interests because of its potential applications to photocatalyst,[2] chemical sensors,[3] solar cell electrodes,[4] and hydrogen storage materials.[5] Titania usually exists in three different forms: anatase (tetragonal, $a = b = 3.78$ Å; $c = 9.50$ Å), rutile (tetragonal, $a = b = 4.58$ Å; $c = 2.95$ Å), and brookite (rhombohedral, $a = 5.43$ Å; $b = 9.16$ Å; $c = 5.13$ Å). These crystalline structures consist of $[TiO_6]^{2-}$ octahedra, which share edges and corners in different manners while keeping the overall stoichiometry as TiO_2.[4-8] Even though anatase has more edges sharing octahedra, the interstitial space between octahedra is larger, which makes rutile denser than anatase (the density of anatase is 3.84 g/cm^3 and that of rutile is 4.26 g/cm^3, respectively).[4-8] Anatase-to-rutile transformation in pure titania usually occurs at 600 to 700 ºC.[9-11] Phase transition to rutile is nonreversible due to the greater thermodynamic stability of rutile phase.[12, 13] Between the two main kinds of crystalline TiO_2, anatase has been confirmed to have quite high photocatalytic activity in the photodegradation of most pollutants,[14,15] while the photocatalytic activity of rutile is still indistinct. Most work has shown that rutile is a very poor photocatalyst.[16] However, it is widely accepted that the mixed phase of titania is beneficial in reducing the recombination of photogenerated electrons and holes, and it always results in an enhancement of photocatalytic activity.[17, 18]

In our work, sulfate was selected as the adjustor in the process of TiO_2 preparation. By simply varying the proportion of anion in the aqueous solution, the controllable crystalline TiO_2 with the high surface area was successfully synthesized at low temperature. To confirm the effect of the crystalline phase distribution on the photocatalytic activity of prepared TiO_2, the photocatalytic activity of TiO_2 with the different contents of anatase and/or rutile was tested for the photodegradation of congo red.

EXPERIMENTAL

1. Preparation of TiO_2 catalysts

The nanocrystalline TiO_2 catalysts reported in this study (see, Table 1) have been prepared by $TiCl_4$ hydrolysis. Titanium tetrachloride (99.9% $TiCl_4$) was used as the main

* Corresponding author: jybae@kmu.ac.kr

starting material without any further purification. A desired amount of $TiCl_4$ was dissolved in double distilled water in an ice-water bath. The concentration of titanium was adjusted to 0.7 M. This aqueous solution was then mixed with the different amount of $(NH_4)_2SO_4$ (for preparation of anatase, mixed phases, and rutile, respectively) in a temperature-controlled bath. The mixture was continuously stirred at 90 °C for 24 h. Subsequently, the precipitated titania was separated from the solution by using centrifugation and repeatedly washed with double distilled water to make $TiO_2 \cdot nH_2O$ that was free of chloride and sulfate ions. The hydrous TiO_2 was dried at 80 °C under vacuum and ground to fine powder. Then the samples were calcined at 400 °C for 3 h.

Table 1

Synthetic conditions and physicochemical properties of TiO_2 catalysts

Sample	SO_4^{2-}/Cl^-	As-synthesized			Calcined			
		Fraction of rutile[a] [%]	Crystallite size of anatase[b] [nm]	Crystallite size of rutile[b] [nm]	Fraction of rutile[a] [%]	Crystallite size of anatase[b] [nm]	Crystallite size of rutile[b] [nm]	Specific surface area [m^2/g]
(a)	0.000	100.0	-	6.7	100.0	-	12.9	89
(b)	0.002	94.8	1.0	6.0	91.4	10.4	10.4	101
(c)	0.004	83.1	4.7	5.6	79.0	9.9	8.7	133
(d)	0.005	46.6	5.6	5.5	29.7	11.9	7.6	146
(e)	0.007	33.3	5.1	4.6	19.7	10.7	7.1	113
(f)	0.008	23.7	5.2	5.7	13.3	10.1	6.6	128
(g)	0.010	10.4	5.8	2.7	4.0	10.6	9.0	164
(h)	0.020	0.0	6.2	-	0.0	7.9	-	166

[a] Calculated by Eq. (1); [b] Calculated by Eq. (2).

2. Catalysts characterization

Powder XRD patterns were collected using the powder diffractometer (PANalytical X'pert PRO MRD) with Cu K_α radiation (40 kV, 25 mA) at 0.02º step size and 1 second step time over the range $20º < 2\theta < 80º$. The samples were prepared as thin layers on metal slides. N_2-adsorption isotherms were measured at 77 K on a nitrogen adsorption apparatus (Quantachrome QUADRASORB SI). The volume of adsorbed N_2 was normalized to standard temperature and pressure. Prior to the experiments, samples were dehydrated at 200 ºC for 2 h. The specific surface area was determined from the linear part of the BET equation (P/P_0 = 0.05-0.30). UV-VIS diffuse reflectance spectra were obtained for the dry-pressed disk samples using the UV-VIS-NIR spectrophotometer (Varian Cary 50G) equipped with an integrating sphere assembly, using $BaSO_4$ as the reflectance sample. The congo red (CR) concentration was measured by UV-absorption spectroscopy using the Shimadzu UV-1601 spectrophotometer.

3. Photodegradation experiment

The congo red was used as a simulated contaminant in this work. The optical setup used for the photon-irradiation experiments consisted of an arc lamp system (Oriel) equipped with a 500 W Hg/Xe lamp (located at 30 cm above the solution) and a dichroic mirror (420-630 nm) for filtering UV radiation. A set of lenses and apertures focused the light onto the open top-end of the continuously stirred batch photoreactor. The cooling water in a pyrex cylindrical jacket under the lamp was used to keep the reaction temperature constant (20 ºC). A volume of 200 mL of CR/water solution with a CR concentration of 50 mg/L together with 0.1 g of titania was transferred to the reactor, corresponding to 0.5 g/L of TiO_2. The mixture was stirred for 30 min in the dark in order to reach the adsorption-desorption equilibrium for CR before illumination. Samples of approximate 5 mL of the stirred slurry were taken at certain time intervals, keeping the titania/solution ratio constant. After recovering the catalyst by centrifugation, the light absorption of the clear solution was measured at the wavelength of 497 nm (λ_{max} for CR). The absorption was converted to the CR concentration referring to the standard curve showing a linear behavior between the concentration and the absorption at this wavelength.

RESULTS AND DISCUSSION

1. Effect of SO_4^{2-}/Cl^- ratio on crystalline TiO_2

The XRD patterns in Figs. 1 and 2 illustrate the crystalline phases of different samples. In these figures, the systems of (a) and (h) are pure rutile and anatase, respectively, while other systems

consist of both anatase and rutile as listed in Table 1. The fractions of the rutile phases decrease in order of (a) to (h). When the ratio of SO_4^{2-} /Cl^- is adjusted to more than 0.20 in the preparation procedure, only the anatase phase can be observed in the TiO_2 powder. In the range of $0.0 < SO_4^{2-}/Cl^- < 0.2$, the fraction of the rutile phase decreases with increasing concentration of SO_4^{2-} in the aqueous solution, and a large amount of SO_4^{2-} will only result in the presence of the anatase phase. From the above results, it suggests that the effect of SO_4^{2-} largely results in the formation of crystalline TiO_2. It has been reported that the presence of SO_4^{2-} accelerated the growth of TiO_2 clusters to anatase.[19] The addition of Cl^- generally favors the formation of rutile crystallites.[20] As a result, different rutile/anatase mixtures can be prepared by changing the proportions of SO_4^{2-} and Cl^- in the aqueous solution.

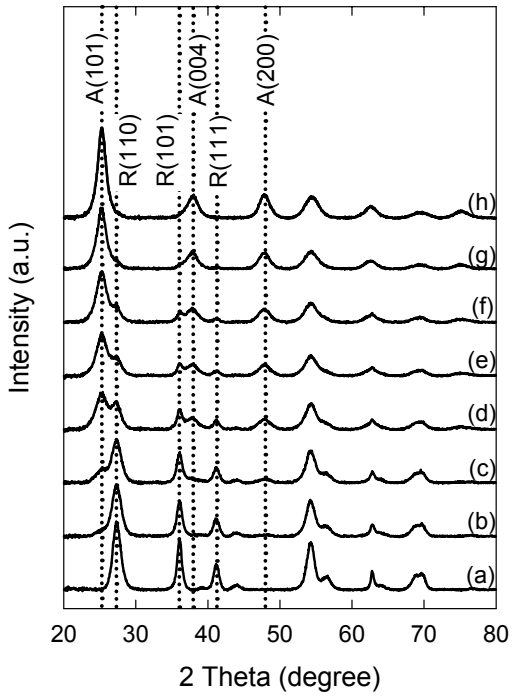

Fig. 1 – XRD patterns for as-synthesized TiO_2 particles. The systems of (a) and (h) are pure rutile and pure anatase, respectively, and the fractions of rutile for (b) to (g) are listed in Table 1.

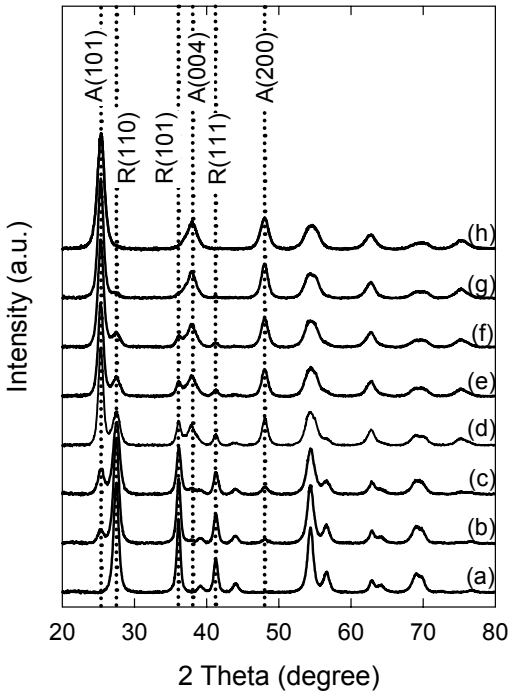

Fig. 2 – XRD patterns for calcined TiO_2 particles. The systems of (a) and (h) are pure rutile and pure anatase, respectively, and the fractions of rutile for (b) to (g) are listed in Table 1.

The fraction of rutile in the samples can be estimated from the corresponding integrated XRD peak intensities using the following equation:[21]

$$\chi = 1/[1+0.8(I_A/I_R)], \quad (1)$$

where χ is the weight fraction of rutile in the powder, and I_A and I_R are the X-ray intensities of the anatase (101) and the rutile (110) peaks, respectively.

The crystallite size of anatase and rutile in the samples are calculated by applying the Debye-Scherrer formula[22] in Eq. (2) on the anatase (101) and rutile (110) diffraction peaks:

$$L = K\lambda/\beta\cos\theta, \quad (2)$$

where L is the crystallite size in angstroms, K is a constant as chosen to be 0.89 here, λ is the wavelength of the X-ray radiation (Cu Kα = 0.15406 nm), β is the corrected band broadening after the subtraction of equipment broadening, and θ is the diffraction angle. The fraction of the rutile phases and crystallite size in the samples are shown in Table 1. The fraction of rutile in calcined samples becomes low in comparison with as-synthesized samples, indicating the structural change from the amorphous to the anatase phase at this calcined temperature.[23]

2. Analysis of UV-VIS diffuse reflectance spectra

UV-VIS spectroscopy has been utilized to characterize the bulk structure of crystalline TiO_2. UV-VIS diffuse reflectance spectroscopy is employed in this work to probe the band structure, or molecular energy levels, since UV-VIS light excitation creates photogenerated electrons and holes. Over the wide ranges of rutile fractions UV-VIS diffuse reflectance spectra are presented in Fig. 3. For the system of (a), *i.e.,* a pure rutile, the significant increasing of the absorption at wavelengths shorter than 413 nm can be assigned to the intrinsic band-gap absorption of rutile. The band gap (E_g) is estimated to be 3.0 eV from the following equation:[24]

$$\alpha(h\nu) = A(h\nu - E_g)^{m/2}, \quad (3)$$

where α is the absorption coefficient, $h\nu$ is the photon energy, and $m = 1$ for the direct transition between bands. The significant absorption of sample (h) for pure anatase started with 387 nm, exhibiting a band-gap value of 3.2 eV. For other samples, the blue shift of the absorption can be clearly observed in Fig. 3, and it is measured for samples (b) to (g), whose band-gap values are 3.01, 3.02, 3.03, 3.04, 3.05, and 3.12 eV, respectively. The order is consistent with decreasing rutile contents in the TiO_2 powder. The result implies that the difference of rutile contents in the TiO_2 powder influence the band-gap value of TiO_2.

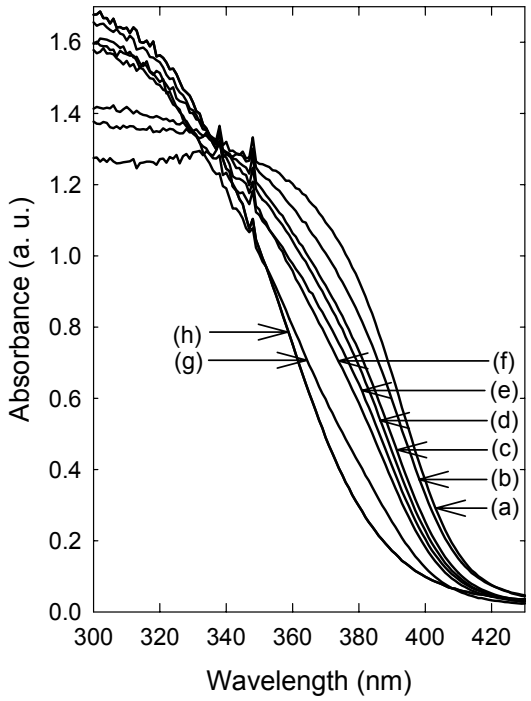

Fig. 3 – UV-VIS diffuse reflectance spectra of calcined TiO_2 particles. The systems (a) to (h) are the same as in Fig. 2.

3. Relationship between crystalline phases and photocatalytic activity

Photocatalytic studies have been carried out by investigating the decomposition reaction of CR in the different contents of rutile. The photodegradation of CR is the pseudo-zero-order reaction. In this case its kinetics can be expressed as $\ln (C_0/C) = kt$, where k is the apparent reaction rate constant, and C_0 and C are the initial concentration and the reaction concentration of CR, respectively. In our experiments, all the solutions for photocatalytic reactions are in the neutral condition, and the changes of pH are found to be relatively small. Figs. 4 and 5 show the CR photodegradation for prepared TiO_2 particles. The photodecomposition rate constants are found to be systematic dependencies, which is not linearly but has certain maximum conditions, e.g., (a) 0.0266 min^{-1}, (b) 0.0291 min^{-1}, (c) 0.0447 min^{-1}, (d) 0.0462 min^{-1}, (e) 0.0476 min^{-1}, (f) 0.0384 min^{-1}, (g) 0.0296 min^{-1}, and (h) 0.0366 min^{-1}. It is considered that the differences in its rate constants are attributed to the crystalline phases, the morphology, and the surface area of the TiO_2 particles.

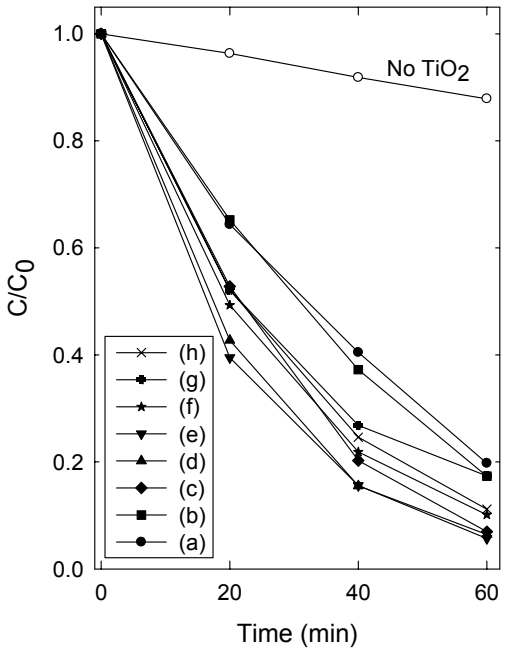

Fig. 4 – Curves for the photocatalytic decomposition of congo red with different calcined TiO_2 catalysts. The systems (a) to (h) are the same as in Fig. 2.

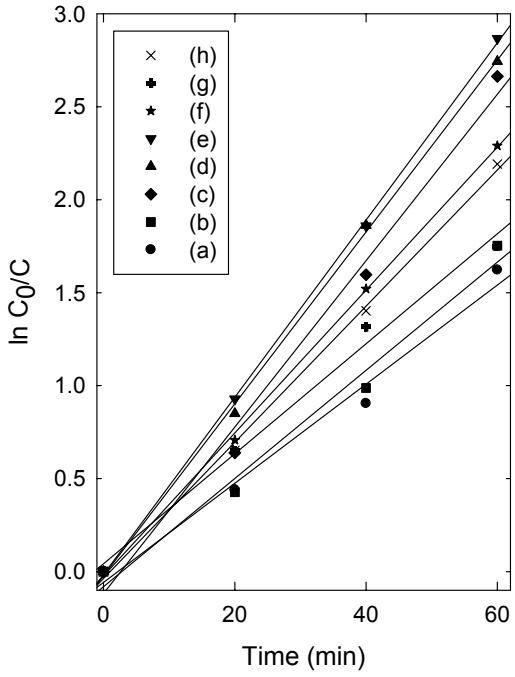

Fig. 5 – Rate constants for the photocatalytic decomposition of congo red with different calcined TiO_2 catalysts. The systems (a) to (h) are the same as in Fig. 2.

If only the surface area is considered, the sample (h) (*ca.* 166 m^2/g) has the larger surface area than others, suggesting that the sample (h) should have better photocatalytic activities. However, the specific surface area of the sample (e) (*ca.* 19.7% rutile) is 113 m^2/g, which is higher than that of the sample (h). This result implies that surface area is not the main factor for photocatalytic activities. In this regard the photocatalytic activity of prepared TiO_2 catalysts is strongly dependent on the crystalline phase. The sample containing 19.7% rutile, *i.e.*, the sample (e), shows the highest photocatalytic activity for CR photodegradation as observed in our experiments. From the above results, the anatase/rutile mixed phase shows the synergistic effect with enhancing the photocatalytic activity.

CONCLUSIONS

Samples with different anatase-to-rutile ratios have been synthesized, and the relationship between the crystalline phase and their activities was investigated. By simply varying the proportion of SO_4^{2-} and Cl^- in the aqueous solution, the different contents of anatase and rutile phases in the powders have been successfully controlled. The different blue shifts of the UV-VIS absorption of the samples are observed because of the different contents of the anatase phase in samples. The catalyst contaning 19.7% rutile shows the highest photocatalytic activity for the photodgradation of CR due to synergistic effects between anatase and rutile.

Acknowledgements. This work was supported by the grant (No. RTI04-01-04) from the Regional Technology Innovation Program of the Ministry of Commerce, Industry and Energy (MOCIE), Korea. Parts of experimental equipments were donated by ATI Korea Co., Ltd.

REFERENCES

1. A. Fujishima and K. Honda, *Nature*, **1972**, *238*, 37.
2. M. R. Hoffmann, S. T. Martin, W. Choi and D. W. Bahnemann, *Chem. Rev.*, **1995**, *95*, 69.
3. M. Kunst, T. Moehl, F. Wunsch and H. Tributsch, *Superlattice Microst.*, **2006**, *39*, 376.
4. S. M. Karvinen, *Ind. Eng. Chem. Res.*, **2003**, *42*, 1035.
5. J. Chen, S. L. Li, Z. L. Tao, Y. T. Shen and C. X. Cui, *J. Am. Chem. Soc.*, **2003**, *125*, 5284.
6. M. Gopal, W. J. M. Chan and L. C. D. Jonghe, *J. Mater. Sci.*, **1997**, *32*, 6001.
7. H. F. Mark, D. F. Othmer, C. G. Overberger and G. T. Seaberg, "Enclyopedia of Chemical Technology", John Wiley, New York, 1983.
8. R. C. Weast, "Handbook of Chemistry and Physics", CRC Press, London, 1984.
9. A. W. Zanderna, C. N. R. Rao and J. M. Honig, *Trans. Faraday Soc.*, **1958**, *54*, 1069.
10. S. R. Yoganarasimhan and C. N. R. Rao, *Trans. Faraday Soc.*, **1962**, *58*, 1579.
11. S. R. Kumar, S. C. Pillai, U. S. Hareesh, P. Mukundan and K. G. K. Warrier, *Mater. Lett*., **2000**, *43*, 286.
12. D. J. Reidy, J. D. Holmes and M. A. Morris, *J. Eur. Cer. Soc.*, **2006**, *26*, 1527.
13. A. Navrotsky and O. J. Kleppla, *J. Am. Cer. Soc.*, **1967**, *50*, 626.
14. J. Zhu, W. Zheng, B. He, J. Zhang and M. Anpo, *J. Mol. Catal. A*, **2004**, *216*, 35.
15. J. Zhang, T. Ayusawa, M. Minagawa, K. Kinugawa, H. Yamashita, M. Matsuoka and M. Anpo, *J. Catal.*, **2001**, *198*, 1.
16. K. Okamoto, Y. Yamamoto, H. Tanaka, M. Tanaka and A. Itaya, *Bull. Chem. Soc. Jpn.*, **1985**, *58*, 2015.
17. R. R. Bacsa and J. Kiwi, *Appl. Catal. B*, **1998**, *16*, 19.
18. M. Yan, F. Chen, J. Zhang and M. Anpo, *J. Phys. Chem. B*, **2005**, *109*, 8673.
19. Q. Zhang, L. Gao and J. Guo, *J. Eur. Cer. Soc.*, **2000**, *20*, 2153.
20. Q. Zhang and L. Gao, *Langmuir*, **2003**, *19*, 967.
21. R. A. Spurr and H. Myers, *Anal. Chem.*, **1957**, *29*, 760.
22. J. Lin, Y. Lin, P. Liu, M. J. Meziani, L. F. Allard and Y. Sun, *J. Am. Chem. Soc.*, **2002**, *124*, 11514.
23. Q. Zhang, L. Gao and J. Guo, *Appl. Catal. B*, **2000**, *26*, 207.
24. E. Sanchez and T. Lopez, *Mater. Lett.*, **1995**, *25*, 271.